Increasing the Open-Circuit Voltage of Photoprotein-Based Photoelectrochemical Cells by Manipulation of the Vacuum Potential of the Electrolytes

Swee Ching Tan,[†,⊥,*] Lucy I. Crouch,[‡,∥] Sumeet Mahajan,[§] Michael R. Jones,[‡] and Mark E. Welland[†]

[†]Nanoscience Centre, University of Cambridge, 11 JJ Thomson Avenue, Cambridge CB3 0FF, U.K., [‡]School of Biochemistry, University of Bristol, Medical Sciences Building, University Walk, Bristol BS8 1TD, U.K., and [§]Cavendish Laboratory, University of Cambridge, JJ Thomson Avenue, Cambridge, CB3 0HE, U.K

ABSTRACT The innately highly efficient light-powered separation of charge that underpins natural photosynthesis can be exploited for applications in photoelectrochemistry by coupling nanoscale protein photoreaction centers to man-made electrodes. Planar photoelectrochemical cells employing purple bacterial reaction centers have been constructed that produce a direct current under continuous illumination and an alternating current in response to discontinuous illumination. The present work explored the basis of the open-circuit voltage (V_{OC}) produced by such cells with reaction center/antenna (RC-LH1) proteins as the photovoltaic component. It was established that an up to ~30-fold increase in V_{OC} could be achieved by simple manipulation of the electrolyte connecting the protein to the counter electrode, with an approximately linear relationship being observed between the vacuum potential of the electrolyte and the resulting V_{OC}. We conclude that the V_{OC} of such a cell is dependent on the potential difference between the electrolyte and the photo-oxidized bacteriochlorophylls in the reaction center. The steady-state short-circuit current (J_{SC}) obtained under continuous illumination also varied with different electrolytes by a factor of ~6-fold. The findings demonstrate a simple way to boost the voltage output of such protein-based cells into the hundreds of millivolts range typical of dye-sensitized and polymer-blend solar cells, while maintaining or improving the J_{SC}. Possible strategies for further increasing the V_{OC} of such protein-based photoelectrochemical cells through protein engineering are discussed.

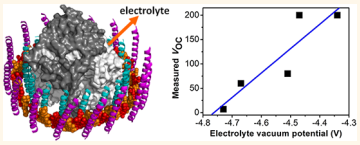

KEYWORDS: photovoltaic · photoelectrochemical cell · enhanced photovoltage · reaction center · electrolyte

It has long been recognized that the natural photovoltaic properties of photosynthetic reaction center (RC) pigment-proteins can be investigated and utilized *in vitro*.[1−3] As well as providing a novel means of generating photocurrents[4−8] and oxidizing or reducing potentials that can be used for photocatalysis,[9] such proteins have properties that could be exploited for the construction of photosensors, biosensors, and elements in logic circuits.[10−16] An advantage of working with natural macromolecules is that the protein assembly machinery of a living cell can be used to construct a very complex, nanoscale photovoltaic material, with the tools of genetic engineering and structural biology enabling modification of that material with a subnanometer precision. In addition the fundamental charge separation process in natural photoreaction centers is extremely efficient in terms of quantum yield,[17] as are the light-harvesting processes that feed the RC with excitation energy.[18]

Studies of how RCs interface with electrodes have focused mainly on the resulting short-circuit photocurrent density (J_{SC}),[4−8] with very little attention paid to the associated open-circuit voltage (V_{OC}). As the efficiency of any solar cell is strongly dependent on both parameters, an understanding the origin of the V_{OC} is of great importance in improving overall performance. Theory and experiment have shown that the V_{OC} of dye-sensitized solar cells is defined by the energy difference between the conduction band of the nanostructured metal oxide film and the redox potential of the electrolyte.[19,20] In recent years considerable efforts have been put into enhancing the V_{OC} of prototype dye-sensitized solar cells,[19,20] a major challenge being to increase the V_{OC} in a way that does not adversely affect the J_{SC} and overall efficiency.[19,20]

Recently we described the construction of photoelectrochemical cells incorporating purple bacterial photosynthetic complexes that produce a conventional direct current (dc) during continuous illumination, and a novel alternating current (ac) in response to discontinuous illumination.[21] Cells were constructed using either RCs or RC-LH1

* Address correspondence to sctan@mit.edu.

Received for review July 25, 2012 and accepted September 25, 2012.

Published online September 25, 2012
10.1021/nn303333e

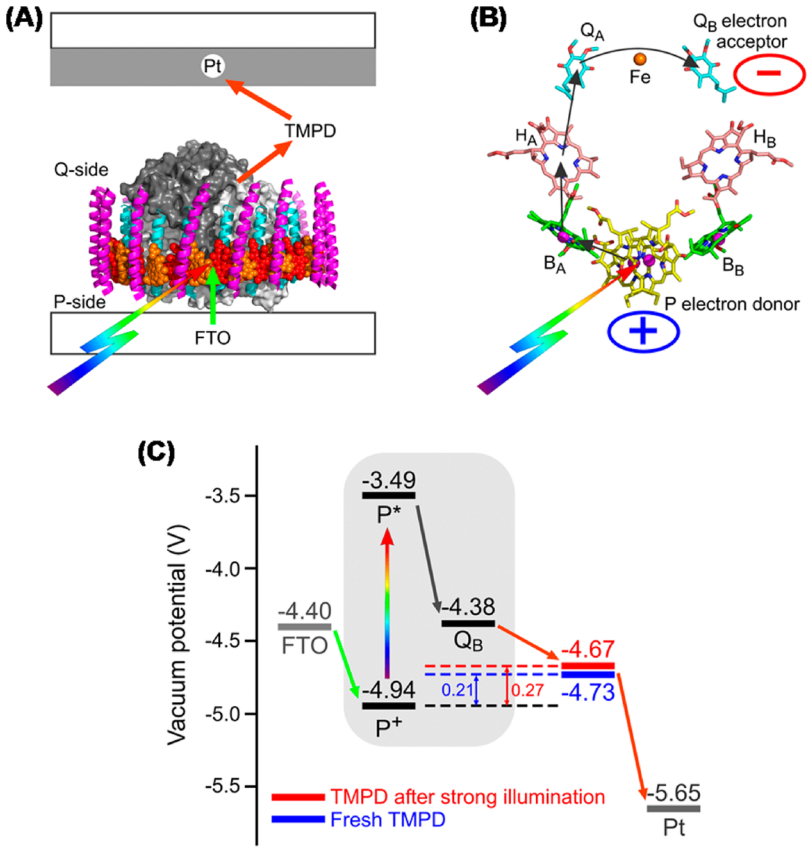

Figure 1. Composition and mechanism of protein photoelectrochemical cell. (A) Output of the RC-LH1 cell is accounted for by photo-oxidized protein complexes being reduced by the transparent FTO-glass anode, with the electrolyte carrying electrons to the Pt cathode. The RC is shown as a solid object in black and white, encircled by an LH1 light-harvesting complex made up of protein (magenta and cyan ribbons) and bacteriochlorophylls (spheres alternating red and orange). (B) Atomic structure of the RC cofactors and mechanism of charge separation. On photoexcitation of a pair of bacteriochlorophylls (P, yellow carbons), an electron is transferred through the protein interior *via* a bacteriochlorophyll (B_A, green carbons), bacteriopheophytin (H_A, pink carbons), and quinone (Q_A, cyan carbons) to the Q_B quinone, creating a charge-separated state $P^+Q_B^-$. (C) Vacuum potentials of key components. The V_{OC} is predicted to be determined by the difference in potential between the P/P^+ couple of the RC (black dashed lines) and the electrolyte (blue dashed lines for fresh TMPD, red dashed lines for aged TMPD). Potentials of the FTO-glass and Pt electrodes are also shown.

proteins, the latter being larger complexes in which the RC is surrounded by a cylinder of LH1 antenna pigment-protein.[22−24] In both cases the redox mediator *N*,*N*,*N*′,*N*′-tetramethyl-*p*-phenylenediamine (TMPD) was used to shuttle electrons from proteins adhered to a conducting fluorine-doped tin oxide (FTO) glass front electrode to a Pt-coated rear electrode, as shown in the schematic of an RC-LH1/TMPD cell in Figure 1A. The process of charge separation within the RC between a pair of bacteriochlorophylls (P) at one end of the protein (P-side) and an acceptor ubiquinone (Q_B) at the other end (Q-side) is also shown (Figure 1B), together with the vacuum potentials of key components in the cell (Figure 1C). The mechanism depicted in Figure 1, in which the photo-oxidized bacteriochlorophyll pair (P^+) is reduced by the FTO electrode (Figure 1A, green arrow) with electrons delivered to the Pt counter electrode by the TMPD electrolyte (Figure 1A, orange arrows), is in accord with the vacuum potentials of these components (Figure 1C). Under continuous illumination, RC-LH1/TMPD cells exposed to continuous illumination produced a J_{SC} that stabilized at approximately 150 nA cm^{-2} after 20 s, RC/TMPD cells producing a similar ∼100 nA cm^{-2} output.[21] Remarkably, when either type of cell was exposed to discontinuous illumination, the external current was found to reverse direction on switching the light from on to off, and this behavior was attributed to a bottleneck in the pathway of electron flow within the cell that resulted in over-reduction of the cofactors of the RC "compartment" and an over-oxidation of the electrolyte (TMPD) "compartment", the reverse current being driven by dissipation of this potential difference.[21]

The present work focuses not on the current output of such cells, but rather on the associated V_{OC}. In principle, the V_{OC} of a cell of the type shown in Figure 1 should depend on the difference in potential between the photo-oxidized primary electron donor, at around −4.94 eV,[25] and the TMPD electrolyte at −4.73 eV[26] (Figure 1C). These are the components that either receive electrons from the FTO anode or donate

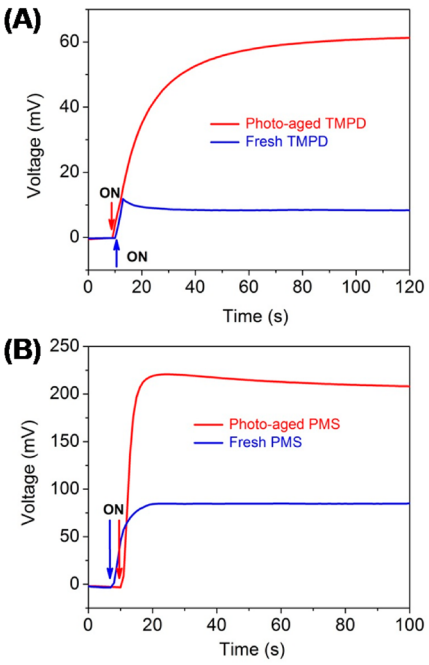

Figure 2. (A) Time dependence of the V_{OC} produced by RC-LH1 cells with fresh or photoaged TMPD under continuous illumination. (B) Time dependence of the V_{OC} produced by RC-LH1 cells with fresh or photoaged PMS under continuous illumination. Arrows indicate the onset of illumination for each trace.

TABLE 1. Characteristics of Protein Photoelectrochemical Cells during Continuous Illumination

cell type	V_{OC} (mV)	mediator potential (eV)	J_{SC} (nA cm^{-2})	electrons produced (nmol min^{-1})[a]	η (%)[b]
RC-LH1/TMPD	7	−4.73	150	0.093	1.05×10^{-5}
RC-LH1/TMPD(aged)	60	−4.67	230	0.131	1.38×10^{-4}
RC-LH1/PMS	80	−4.51	900	0.560	7.20×10^{-4}
RC-LH1/PMS(aged)	205	−4.34/−4.47	750	0.473	1.54×10^{-3}

[a] Calculated according to Bora *et al.*[28]. [b] Calculated from the product of V_{OC} and J_{SC}, divided by the incident light intensity.

electrons to the Pt cathode, and the difference in their midpoint redox potentials gives a theoretical V_{OC} of ~0.21 V (gap between black and blue dotted lines in Figure 1C). However in our previous report the measured V_{OC} was only 0.007 V for RC-LH1/TMPD cells,[21] raising the question of what actually defines the V_{OC}. In the following we examine whether this V_{OC} can be increased through manipulation of a known parameter such as the vacuum potential of the electrolyte.

RESULTS

Figure 2A (blue) shows data for a RC-LH1/TMPD cell of the type described above, producing a steady V_{OC} of ~7 mV under continuous illumination. Typical values for V_{OC} and J_{SC} produced by cells of this type are collated in Table 1. Strong illumination of TMPD for a prolonged period is known to induce a chemical

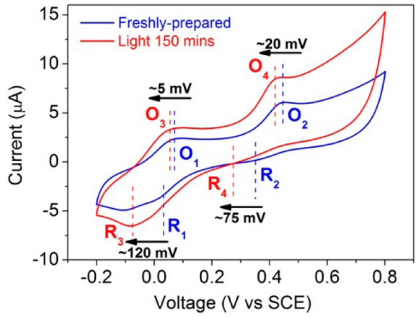

Figure 3. Cyclic voltammogram for TMPD before and after exposure to light at 90 mW cm^{-2} for 150 min. The midpoint potentials of the first and second pair of redox couples before exposing TMPD to light were 0.045 and 0.405 V (*vs* SCE). After 150 min of illumination these potentials shifted to −0.015 and 0.371 V, respectively.

change that alters its reduction potentials, giving an opportunity to test the origins of the V_{OC} produced by this type of cell. Figure 3 shows a cyclic voltammogram for a freshly prepared solution of TMPD (blue) and the same solution after exposure to white light at an intensity of 90 mW cm^{-2} for 150 min (red); this illumination was 9-fold more intense than that used for measurements of photocurrents and photovoltages. After 150 min of illumination the four peaks corresponding to the oxidation and reduction potentials of the first and second redox pair had all shifted toward more negative potentials, irradiation changing the midpoint potential for the first redox pair by ~60 mV to −0.015 V (*vs* SCE). This is the pair relevant to operation of the cell, its redox potential corresponding to a vacuum potential of −4.67 eV.

According to the reasoning presented above, a shift of vacuum potential from −4.73 eV for freshly prepared TMPD/TMPD$^+$ to −4.67 eV for "photo-aged" electrolyte should result in an increase in the theoretical V_{OC} from 0.21 to 0.27 V (Figure 1C, red). Accordingly, a RC-LH1 cell was constructed containing TMPD that had been pre-exposed to 150 min of strong illumination. This cell produced a steady-state V_{OC} of ~60 mV (Figure 2A, red), some 53 mV higher than typically observed for an equivalent cell constructed from freshly prepared TMPD (Figure 2A, blue) and largely matching the predicted change in V_{OC} of ~60 mV. This provided good indications that the V_{OC} of these protein-based photoelectrochemical cells is indeed dependent on the redox potential of the electrolyte. In addition to this marked increase in steady-state V_{OC}, RC-LH1 cells prepared with photoaged TMPD showed a much slower buildup of V_{OC} than cells prepared with fresh TMPD (Figure 2A, red compared with blue).

Examination of the current density under short-circuit conditions showed that RC-LH1 cells containing photoaged TMPD typically produced a steady J_{SC} of approximately 230 nA cm^{-2}, some 80 nA cm^{-2} greater than was typically observed in cells containing freshly prepared TMPD (Figure 4A, red and blue, respectively),

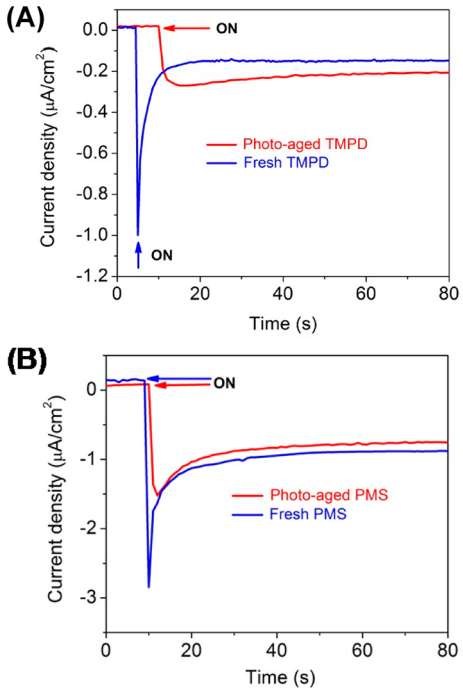

Figure 4. (A) Time dependence of the J_{SC} produced by RC-LH1 cells with fresh or photoaged TMPD under continuous illumination. (B) Time dependence of the J_{SC} from RC-LH1 cells with fresh or photoaged PMS under continuous illumination.

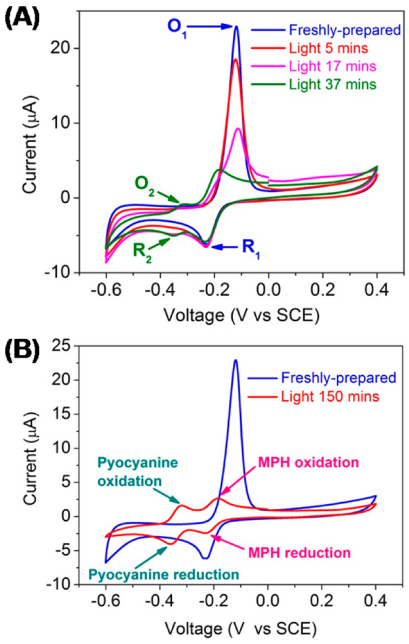

Figure 5. (A) Cyclic voltammetry of PMS before and during the first 37 min of exposure to light at 90 mW cm^{-2}. Peaks corresponding to PMS (O_1 and R_1) decreased, with two new peaks attributable to pyocyanine (O_2 and R_2) appearing after ~17 min (midpoint potential of *ca.* −0.34 V (*vs* SCE)). (B) Voltammograms before and after 150 min of illumination. The oxidation and reduction peaks of pyocyanine and MPH increased in amplitude over the remaining period.

with a strong attenuation of the initial (~0.9 μA cm^{-2}) spike of current flow after turning on the light. Taken together, these changes in time-dependence and amplitude of V_{OC} and J_{SC} indicated differences in the kinetics of interaction of fresh and photoaged TMPD with the RC-LH1 protein and the Pt counter electrode.

RC-LH1 cells were also constructed using phenazine methosulfate (PMS) in place of TMPD. Cyclic voltammetry established that, when freshly prepared, PMS had a midpoint potential of −177 mV (*vs* SCE), in good agreement with literature values.[27] This is equivalent to −4.51 eV in the vacuum level, which in principle could lead to a larger V_{OC} (0.43 V) than cells containing either fresh TMPD or photoaged TMPD. The steady-state V_{OC} of RC-LH1/PMS cells (Figure 2B, blue) was typically ~80 mV under the same illumination conditions as applied to the RC-LH1/TMPD cells, once again supporting the idea that the redox potential difference between the electrolyte and primary electron donor in the RC was a major determinant of the V_{OC} of the cell. The J_{SC} of a typical RC-LH1/PMS cell was approximately 900 nA cm^{-2} (Figure 4B, blue), almost six times larger than that of an equivalent TMPD-containing cell; as shown in Table 1 this current density equated to 0.56 nmol of electrons produced during a steady state of 1 min through photoactivation of the RC-LH1 complexes based on the calculation method described by Bora *et al.*[28]

PMS, the methyl sulfate salt of 5-methylphenazinium (MPH),[29−31] has not previously been used as an electrolyte for a protein photoelectrochemical cell because when exposed to strong illumination, it undergoes a photodegradation process to a mixture of 5-methylphenazine-1-one (pyocyanine) and MPH, the proportions depending on precise conditions.[29−31] In the present work, illumination of a solution of PMS with white light at 90 W cm^{-2} for a period of 150 min was accompanied by extensive changes to the waveform of its cyclic voltammogram (Figure 5). Peaks corresponding to PMS (O_1 and R_1 in Figure 5A, blue) decreased rapidly, with a new pair of peaks becoming visible by around 37 min (O_2 and R_2 in Figure 5A, green). The midpoint potential of this newly formed redox couple was around −0.34 V (*vs* SCE), consistent with new species being pyocyanine.[27,29−34] The initial and final voltammograms after 150 min illumination are compared in Figure 5B; the differences in line shape were consistent with photodecomposition of PMS (−4.51 eV) into a mixture of pyocyanine (at −4.34 eV)[27] and MPH (at −4.47 eV).

Aliquots of this photodegraded PMS solution were also used as the electrolyte in a RC-LH1 cell. The J_{SC} observed, around 750 nA cm^{-2} (Figure 4B, red), was a little lower than the ~900 nA cm^{-2} obtained from a RC-LH1 cell containing fresh PMS (Figure 4B, blue). However the steady V_{OC} of the cell constructed with photodegraded PMS was 205 mV, more than twice that obtained with cells made with freshly prepared PMS (Figure 2B, red compared with blue). Again, this

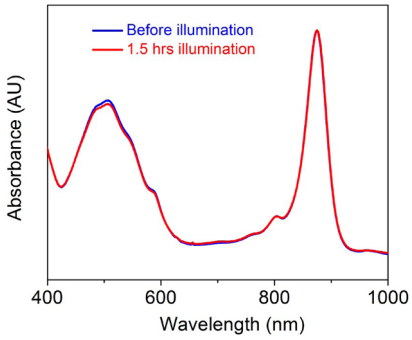

Figure 6. Normalized absorbance spectra of RC-LH1 complexes in solution before (blue) and after (red) 1.5 h of exposure to the same 90 mW cm^{-2} light source used to photoage PMS and TMPD.

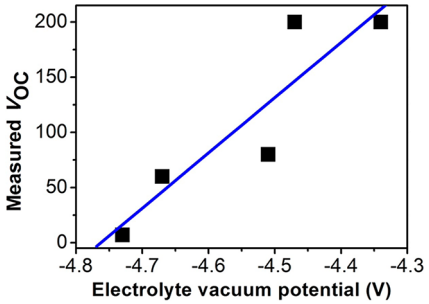

Figure 7. Relationship between vacuum potential of electrolyte and the observed V_{OC}. Two data points are included for cells incorporating photoaged PMS, corresponding to the reduction potentials of pyocyanine and MPH (see Table 1).

was in line with expectations that a mixture of pyocyanine and MPH should give a V_{OC} that is higher (by between 40 and 170 mV depending on relative amounts) than the ~80 mV obtained with PMS.

It should be stressed that the photoaging of TMPD or PMS described above was carried out before the construction of a photoelectrochemical cell, and so the effects of this illumination on the output of the cell were a consequence of changes in the properties of the electrolyte and not a change in the properties of the RC-LH1 complex. Figure 6 shows that the absorbance spectrum of the RC-LH1 complex in Tris-HCl buffer was essentially unchanged after exposure to continuous illumination over a period of 90 min from the 90 mW cm^{-2} light source used to photoage TMPD or PMS. In this spectrum the major band at 875 nm is attributed to the LH1 antenna, and the small bands at 800 and 760 nm are attributed to the RC. Degradation of the complex would be expected to result in a drop in the intensity of these bands and the appearance of the absorbance band of free bacteriochlorophyll at around 760 nm, but this was not seen.

As has been commented on previously,[35] the acquisition of standard $I-V$ curves for these protein-based cells was problematic due to the transient nature of the voltage and current outputs. Accordingly, an estimation of the relative steady-state external power conversion efficiency (η) of these cells was made by multiplying the steady-state J_{SC} by the steady-state V_{OC} and dividing by the intensity of the light reaching the external surface of the cell (*i.e.*, carrying out a version of the standard calculation but without the fill factor that would be estimated from a full $I-V$ curve).[35] The resulting overall efficiencies of the four cells are listed in Table 1. Even though the highest photocurrent was produced from the cell with fresh PMS, the highest efficiency was achieved by the cell with aged PMS due to the ~2.5-fold larger V_{OC}.

DISCUSSION

The data outlined above demonstrate that it is possible to bring about a ~30-fold increase in the V_{OC} of a photoelectrochemical cell based on purple bacterial RC-LH1 complexes by simple manipulation of the electrolyte (Table 1). The V_{OC} scaled approximately linearly with the measured potential of the electrolyte (Figure 7), supporting the idea that it is dependent on the potential difference between the electrolyte and the P/P$^+$ redox couple in the protein. The largest value obtained, 205 mV for a cell in which the electrolyte was photodegraded PMS, was very high for a protein-based cell, being around a third of the open-circuit voltage typical of dye-sensitized solar cells.[19]

The fact that the V_{OC} produced by RC-LH1 cells could be increased so dramatically through such simple manipulation of the electrolyte is very encouraging and suggests that additional increases could be brought about. One possibility would be to further lower the redox potential of the electrolyte, but a limitation is that use of electrolytes with significantly lower potentials than that of the Q_B ubiquinone could impair electron transfer between the RC and the counter electrode. However this restriction could be overcome if the multistep electron transfer through the RC could be tapped into at an earlier stage than the terminal quinone acceptor at Q_B (Figure 1b), such that electrons leave the complex at a much more reducing potential.

A second possibility is to alter the potential of the P/P$^+$ redox couple through protein engineering, and indeed it is known that site-directed mutagenesis of just four amino acids can modulate this redox potential over a range of almost 400 mV, with an RC having been reported in which the P/P$^+$ potential is around 300 mV above that in the native RC.[36,37] According to the scheme in Figure 1B, such a mutant would be expected to have a vacuum potential of around −5.24 eV and so produce a much larger V_{OC}. It seems entirely possible that through a combination of changes to the electrolyte and redox centers inside the RC it will be possible to boost the V_{OC} of these protein-based photoelectrochemical cells into the several hundreds of millivolts range commonly obtained in dye-sensitized solar cells.

Turning to the J_{SC} output, replacing the TMPD in RC-LH1 cells with PMS increased the J_{SC} by a factor of 6, and photodegraded PMS also produced a larger current than TMPD (Table 1). These findings suggest that it should be possible to further increase J_{SC} through the selection of the most appropriate electrolyte. However, perhaps the most obvious route to increasing the current output into the mA cm^{-2} range typical for dye-sensitized solar cells will be to optimize coverage of the photoactive protein on the electrode surface through more controlled deposition, possibly exploiting the natural ability of many photosynthetic proteins to self-assemble in 2D arrays, and to move from using 2D planar electrodes to 3D nanostructured electrodes. A complex, 3D structure for the interface between the photovoltaic component and the adjacent electron-accepting or electron-donating conducting surface is a common characteristic of the most efficient dye-sensitized solar cells.

CONCLUSIONS

It has been demonstrated that the V_{OC} of solar cells incorporating a photosynthetic protein as the photovoltaic material can be increased significantly in a way that also brings about increases in J_{SC}. We conclude that the V_{OC} of such a cell is dependent on the potential difference between the electrolyte and the P/P^+ redox couple in the reaction center. This finding provides a basic understanding of the origin of the V_{OC} of such cells, as well as providing indications of how this parameter can be further boosted through protein engineering to the levels achieved routinely in dye-sensitized solar cells.

MATERIALS AND METHODS

Cell Fabrication. PufX-deficient RC-LH1 proteins from *Rhodobacter sphaeroides* were isolated as described in detail recently[21] and stored at −80 °C until used. Cells comprised a front electrode formed from a 20 mm × 20 mm × 2.2 mm piece of FTO conducting glass (TEC 15 ohm/sq; Solaronix, Switzerland) and a back electrode formed from a second piece of FTO conducting glass of the same dimensions (TEC 7 ohm/sq) covered by an approximately 25 nm thick layer of Pt deposited by a dc magnetron sputtering system. All FTO-glass substrates were sonicated with acetone and then 2-propanol and then underwent a UV/ozone cleaning process. The two electrodes were joined using a U-shaped piece of 75 μm thick hot-melt sealing foil (Dupont), forming a cavity into which was injected 10 μL of a mixture of protein and electrolyte at final concentrations 85 and 250 μM, respectively. The opening was then sealed with a rapid setting epoxy (Araldite).

Electrical Measurements and Cyclic Voltammetry. Photochronoamperometry was performed as described previously[21] using light from a 100 W incandescent lamp passed through a 570 nm long-pass filter to give an incident intensity of 10 mW cm^{-2}. All photocurrents and photovoltages were recorded using a 2636A SourceMeter (Keithley).

To investigate the effect of strong light on TMPD or PMS, cyclic voltammetry (CV) was used to study changes in their redox potentials during continuous illumination from a 100 W incandescent lamp. Electrochemical analysis was performed using an Autolab PGSTAT302N potientiostat with a three-electrode system. The working electrode was a 1.0 mm diameter platinum disk, the counter electrode was a platinum wire mesh, and the reference was a saturated calomel electrode (SCE). Prior to the experiments the counter electrode was washed with sulfuric acid and the working electrode was polished with a small amount of alumina powder on a felt polishing pad. Both electrodes were then rinsed thoroughly with distilled water. The three electrodes were immersed in a glass cell containing 10 mL of 0.5 mM TMPD or PMS in a buffer comprising 200 mM Tris-HCl (pH 8.0), and CV measurements were performed under a nitrogen atmosphere with an incident light intensity of 90 mW cm^{-2}.

Conflict of Interest: The authors declare no competing financial interest.

[⊥]Present address: Department of Materials Science and Engineering, Massachusetts Institute of Technology, 77 Massachusetts Avenue, Cambridge, MA 02139, United States. [∥]Present address: Department of Pharmacology, University of Cambridge, Tennis Court Road, Cambridge, CB2 1PD, United Kingdom.

Acknowledgment. S.C.T. would like to acknowledge scholarships from Cambridge Commonwealth Trust and Wingate Foundation. L.I.C. and M.R.J. acknowledge funding from the Biotechnology and Biological Sciences Research Council of the United Kingdom.

REFERENCES AND NOTES

1. Drachev, L. A.; Kondrashin, A. A.; Samuilov, V. D.; Skulachev, V. P. Generation of Electric Potential by Reaction Center Complexes from *Rhodospirillum rubrum*. *FEBS Lett.* **1975**, *50*, 219–222.
2. Schönfeld, M.; Montal, M.; Feher, G. Functional Reconstitution of Photosynthetic Reaction Centers in Planar Lipid Bilayers. *Proc. Natl. Acad. Sci. U. S. A.* **1979**, *76*, 6351–6355.
3. Janzen, A. F.; Seibert, M. Photoelectrochemical Conversion Using Reaction Center Electrodes. *Nature* **1980**, *286*, 584–585.
4. Lebedev, N.; Trammell, S. A.; Spano, A.; Lukashev, E.; Griva, I.; Schnur, J. Conductive Wiring of Immobilized Photosynthetic Reaction Center to Electrode by Cytochrome *c*. *J. Am. Chem. Soc.* **2006**, *128*, 12044–12045.
5. Xu, J.; Lu, Y.; Liu, B.; Xu, C.; Kong, J. Sensitively Probing the Cofactor Redox Species and Photo-Induced Electron Transfer of Wild-Type and Pheophytin-Replaced Photosynthetic Proteins Reconstituted in Self-Assembled Monolayers. *J. Solid State Electrochem.* **2007**, *11*, 1689–1695.
6. Ham, M. H.; Choi, J. H.; Boghossian, A. A.; Jeng, E. S.; Graff, R. A.; Heller, D. A.; Chang, A. C.; Mattis, A.; Bayburt, T. H.; Grinkova, Y. V.; *et al*. Photoelectrochemical Complexes for Solar Energy Conversion that Chemically and Autonomously Regenerate. *Nat. Chem.* **2010**, *2*, 929–936.
7. Lu, Y. D.; Yuan, M. J.; Liu, Y.; Tu, B.; Xu, C. H.; Liu, B. H.; Zhao, D. Y.; Kong, J. L. Photoelectric Performance of Bacteria Photosynthetic Proteins Entrapped on Tailored Mesoporous WO_3-TiO_2. Films. *Langmuir* **2005**, *21*, 4071–4076.
8. Trammell, S. A.; Spano, A.; Price, R.; Lebedev, N. Effect of Protein Orientation on Electron Transfer between Photosynthetic Reaction Centers and Carbon Electrodes. *Biosens. Bioelectron.* **2006**, *21*, 1023–1028.
9. Krassen, H.; Schwarze, A.; Friedrich, B.; Ataka, K.; Lenz, O.; Heberle, J. Photosynthetic Hydrogen Production by a Hybrid Complex of Photosystem I and [NiFe]-Hydrogenase. *ACS Nano* **2009**, *3*, 4055–4061.
10. Nishihara, H.; Kanaizuka, K.; Nishimori, Y.; Yamanoi, Y. Construction of Redox- and Photo-Functional Molecular Systems on Electrode Surface for Application to Molecular Devices. *Coord. Chem. Rev.* **2007**, *251*, 2674–2687.

11. Terasaki, N.; Yamamoto, N.; Tamada, K.; Hattori, M.; Hiraga, T.; Tohri, A.; Sato, I.; Iwai, M.; Iwai, M.; Taguchi, S.; *et al*. Bio-Photo Sensor: Cyanobacterial Photosystem I Coupled with Transistor via Molecular Wire. *Biochim. Biophys. Acta* **2007**, *1767*, 653–659.
12. Frolov, L.; Rosenwaks, Y.; Richter, S.; Carmeli, C.; Carmeli, I. Photoelectric Junctions between GaAs and Photosynthetic Reaction Center Protein. *J. Phys. Chem. C* **2008**, *112*, 13426–13430.
13. Giardi, M. T.; Scognamiglio, V.; Rea, G.; Rodio, G.; Antonacci, A.; Lambreva, M.; Pezzotti, G.; Johanningmeier, U. Optical Biosensors for Environmental Monitoring Based on Computational and Biotechnological Tools for Engineering the Photosynthetic D1 Protein of *Chlamydomonas reinhardtii*. *Biosens. Bioelectron.* **2009**, *25*, 294–300.
14. Sanders, C. A.; Rodriguez, M.; Greenbaum, E. Stand-Off Tissue-Based Biosensors for the Detection of Chemical Warfare Agents Using Photosynthetic Fluorescence Induction. *Biosens. Bioelectron.* **2001**, *16*, 439–446.
15. Scognamiglio, V.; Pezzotti, G.; Pezzotti, I.; Cano, J.; Buonasera, K.; Giannini, D.; Giardi, M. T. Biosensors for Effective Environmental and Agrifood Protection and Commercialization: From Research to Market. *Microchim. Acta* **2010**, *170*, 215–225.
16. Ventrella, A.; Catucci, L.; Agostiano, A. Herbicides Affect Fluorescence and Electron Transfer Activity of Spinach Chloroplasts, Thylakoid Membranes and Isolated Photosystem II. *Bioelectrochemistry* **2010**, *79*, 43–49.
17. Jones, M. R. The Petite Purple Photosynthetic Powerpack. *Biochem. Soc. Trans.* **2009**, *37*, 400–407.
18. Van Grondelle, R.; Dekker, J. P.; Gillbro, T.; Sundstrom, V. Energy Transfer and Trapping in Photosynthesis. *Biochim. Biophys. Acta, Bioenerg.* **1994**, *1187*, 1–65.
19. O'Regan, B.; Gratzel, M. A Low-Cost, High-Efficiency Solar-Cell Based on Dye-Sensitized Colloidal TiO_2 Films. *Nature* **1991**, *352*, 737–740.
20. Bisquert, J.; Cahen, D.; Hodes, G.; Ruhle, S.; Zaban, A. Physical Chemical Principles of Photovoltaic Conversion with Nanoparticulate, Mesoporous Dye-Sensitized Solar Cells. *J. Phys.Chem. B* **2004**, *108*, 8106–8118.
21. Tan, S. C.; Crouch, L. I.; Jones, M. R.; Welland, M. E. Generation of Alternating Current in Response to Discontinuous Illumination by Novel Photoelectrochemical Cells Based on Photosynthetic Proteins. *Angew. Chem., Int. Ed.* **2012**, *51*, 6667–6671.
22. Roszak, A. W.; Howard, T. D.; Southall, J.; Gardiner, A. T.; Law, C. J.; Isaacs, N. W.; Cogdell, R. J. Crystal Structure of the RC-LH1 Core Complex from *Rhodopseudomonas palustris*. *Science* **2003**, *302*, 1969–1972.
23. Fotiadis, D.; Qian, P.; Philippsen, A.; Bullough, P. A.; Engel, A.; Hunter, C. N. Structural Analysis of the Reaction Center Light-Harvesting Complex I Photosynthetic Core Complex of *Rhodospirillum rubrum* Using Atomic Force Microscopy. *J. Biol. Chem.* **2004**, *279*, 2063–2068.
24. Qian, P.; Bullough, P. A.; Hunter, C. N. Three-Dimensional Reconstruction of a Membrane-Bending Complex - The RC-LH1-PufX Core Dimer of *Rhodobacter sphaeroides*. *J. Biol. Chem.* **2008**, *283*, 14002–14011.
25. Visschers, R. W.; Vulto, S. I. E.; Jones, M. R.; van Grondelle, R.; Kraayenhof, R. Functional LH1 Antenna Complexes Influence Electron Transfer in Bacterial Photosynthetic Reaction Centers. *Photosynth. Res.* **1999**, *59*, 95–104.
26. Wardman, P. Reduction Potentials of One-Electron Couples Involving Free-Radicals in Aqueous Solution. *J. Phys. Chem. Ref. Data* **1989**, *18*, 1637–1755.
27. Chew, V. S. F.; Bolton, J. R. Photochemistry of 5-Methylphenazinium Salts in Aqueous-Solution - Products and Quantum Yield of the Reaction. *J. Phys. Chem.* **1980**, *84*, 1903–1908.
28. Bora, D. K.; Rozhkova, E. A.; Schrantz, K.; Wyss, P. P.; Braun, A.; Graule, T.; Constable, E. C. Functionalization of Nanostructured Hematite Thin-Film Electrodes with the Light-Harvesting Membrane Protein C-Phycocyanin Yields Enhanced Photocurrent. *Adv. Funct. Mater.* **2012**, 490–502.
29. Zaugg, W. S. Spectroscopic Characteristics and Some Chemical Properties of N-Methylphenazinium Methyl Sulfate (Phenazine Methosulfate) and Pyocyanine at Semiquinoid Oxidation Level. *J. Biol. Chem.* **1964**, *239*, 3964–3970.
30. Halaka, F. G.; Babcock, G. T.; Dye, J. L. Properties of 5-Methylphenazinium Methyl Sulfate - Reaction of the Oxidized Form with NADH and of the Reduced Form with Oxygen. *J. Biol. Chem.* **1982**, *257*, 1458–1461.
31. Prince, R. C.; Linkletter, S. J. G.; Dutton, P. L. The Thermodynamic Properties of Some Commonly Used Oxidation-Reduction Mediators, Inhibitors and Dyes, as Determined by Polarography. *Biochim. Biophys. Acta, Bioenerg.* **1981**, *635*, 132–148.
32. Morrison, M. M.; Seo, E. T.; Howie, J. K.; Sower, D. T. Flavin Model Systems 0.1. Electrochemistry of 1-Hydroxy-Phenazine and Pyocyanine in Aprotic Solvents. *J. Am. Chem. Soc.* **1978**, *100*, 207–211.
33. Sanderson, D. G.; Gross, E. L.; Seibert, M. A Photosynthetic Photoelectrochemical Cell using Phenazine Methosulfate and Phenazine Ethosulfate as Electron-Acceptors. *Appl. Biochem. Biotechnol.* **1987**, *14*, 1–14.
34. Xu, X.; Zhao, J. Q.; Jiang, D. C.; Kong, J. L.; Liu, B. H.; Deng, J. Q. TiO_2 Sol-Gel Derived Amperometric Biosensor for H_2O_2 on the Electropolymerized Phenazine Methosulfate Modified Electrode. *Anal. Bioanal. Chem.* **2002**, *374*, 1261–1266.
35. Ciesielski, P. N.; Hijazi, F. M.; Scott, A. M.; Faulkner, C. J.; Beard, L.; Emmett, K.; Rosenthal, S. J.; Cliffel, D.; Jennings, G. K. Photosystem I - Based Biohybrid Photoelectrochemical Cells. *Biores. Technol.* **2010**, *101*, 3047–3053.
36. Allen, J. P.; Williams, J. C. Relationship between the Oxidation Potential of the Bacteriochlorophyll Dimer and Electron-Transfer in Photosynthetic Reaction Centers. *J. Bioenerg. Biomembr.* **1995**, *27*, 275–283.
37. Spiedel, D.; Jones, M. R.; Robert, B. Tuning of the Redox Potential of the Primary Electron Donor in Reaction Centres of Purple Bacteria: Effects of Amino Acid Polarity and Position. *FEBS Lett.* **2002**, *527*, 171–175.